mathematics

Article

Synchronized Rhythmic Activity of Ants with Distributed Rest Periods

Pedro M. M. da Silveira and José F. Fontanari *

Instituto de Física de São Carlos, Universidade de São Paulo, Caixa Postal 369, São Carlos 13560-970, SP, Brazil; pmasotti@usp.br
* Correspondence: fontanari@ifsc.usp.br

Abstract: Synchronization is a prevalent phenomenon in biological systems, including social insects such as ants. Certain ant species exhibit remarkable synchronization of their activities within the nest. To elucidate the underlying mechanisms of this coordinated behavior, we propose an integro-differential equation model that captures the autocatalytic nature of ant activation. Active ants can stimulate inactive individuals, leading to a cascade of arousal. By incorporating a stochastic component to represent variability in rest periods, we explore the conditions necessary for synchronization. Our analysis reveals a critical threshold for fluctuations in rest duration. Exceeding this threshold disrupts synchronization, driving the system towards a stable equilibrium. These findings offer valuable insights into the factors governing ant activity synchronization and highlight the delicate balance between model parameters required to generate rhythmic patterns.

Keywords: synchronization; collective behavior; functional equations; fixed-point analysis

MSC: 34K24; 37N25; 34K60

Citation: da Silveira, P.M.M.; Fontanari, J.F. Synchronized Rhythmic Activity of Ants with Distributed Rest Periods. *Mathematics* **2024**, *12*, 3893. https://doi.org/10.3390/math12243893

Academic Editors: Daniele Fournier-Prunaret and José Leonel Linhares da Rocha

Received: 22 October 2024
Revised: 5 December 2024
Accepted: 9 December 2024
Published: 10 December 2024

1. Introduction

Endogenous synchronization arises from internal mechanisms within a system, i.e., it is generated by the interactions and dynamics of the components within the system itself, rather than being driven by external signals or influences. It is the source of remarkable displays of self-organization in the biological world, from the cellular to the organismal to the ecological level. Heart cells synchronize their contractions, certain species of fireflies synchronize their flashing patterns, and predator and prey populations often exhibit synchronized cycles [1,2]. Although less appealing than thousands of fireflies flashing in unison, the synchronized bursts of activity in the nests of some ant species (e.g., *Leptothorax acervorum*), occurring about three or four times an hour and involving the entire nest population, is an equally fascinating manifestation of endogenous synchronization [3–6]. An evolutionary explanation for the existence of these short-term activity cycles is that they may improve physical access to all parts of the nest, since inactive ants may act as immobile obstacles to moving ants, promoting more efficient brood care [7,8].

A great deal of our knowledge about synchronization comes from the study of coupled oscillators, where each oscillator begins with its own intrinsic natural frequency but changes frequency through interactions with other oscillators [9]. The autocatalytic ant colony model, introduced in the late 1980s to explain bursts of synchronized activity in ant nests [10], follows this prescription: the model assumes a rest period τ that is the same for all ants, introducing a natural time scale into the system. Ants are inactive (asleep) during the rest period, and once this period is over, they are deterministically awake but remain immobile (activatable inactive). Activatable inactive ants become active at a fixed rate and active ants become inactive at another fixed rate. In this scenario of independent ants, the resting times rapidly desynchronize and, at equilibrium, the ants become active (and inactive) at random times so that the proportion of active ants tends to a stationary, time-independent value.

However, when interactions are taken into account by considering the empirical observation that ants are stimulated to become active by nest mates [3–6], Monte Carlo simulations [10] and process algebra [11] indicate that the autocatalytic ant colony model appears capable of generating synchronized bursts of activity. These findings have recently been confirmed by the analytical study of a set of delay differential equations that accurately describe the Monte Carlo simulations in the limit of very large nest sizes [12]. In particular, stable limit-cycle solutions appear when the rest period is greater than a threshold and the ratio of contagious activation to spontaneous activation is sufficiently large.

Here, we build on the analytical formulation of the autocatalytic ant colony model [12] to study the case where the rest periods are random variables, i.e., τ not only varies from ant to ant, but changes each time an ant becomes inactive according to the probability distribution $p(\tau)$. This is a more realistic scenario than that of uniform τ, since the duration of rest periods has been observed to vary between species and can be highly variable within the same species [6]. In addition, the validity of the model predictions for fixed τ depends on their robustness to the effect of noise on the rest period, which is the focus of this study.

We show that when the rest periods are exponentially distributed, the resulting integro-differential equations describing the time dependence of the fraction of ants in different states have no periodic solutions. The only stationary solutions are time-independent solutions that depend only on the mean of the rest period distribution. However, for the zero-truncated normal distribution, which is more adequate to study the effect of noise on the results for a fixed rest period, we find periodic solutions when the noise parameter is below a threshold. To illustrate the complexity resulting from the ant interactions, which are such that the activation rate increases with the number of active ants (hence, the autocatalytic attribute), we note that both too weak and too strong interactions do not produce synchronization. The periodic solutions of the integro-differential equations are the result of a delicate balance of the model parameters, which can only be revealed by the stability analysis of the equilibrium solutions. We note that the autocatalytic ant colony model is not the only model that can explain the emergence of the short-term activity cycles observed in ant nests. For example, there is a class of models that assume that the cycles are caused by the need for energy (food) to meet the demands of the nest [13] (see also [14]). However, the parameters of these models do not have as clear a biological interpretation as those of the autocatalytic ant colony model.

Our goal is to study the mechanisms of synchronization in ant nests using an analytically solvable mathematical model [12]. As noted above, in the autocatalytic ant colony model, both internal clocks and social interactions are required to explain the synchronized bursts of activity in ant nests, and we explore the nontrivial interplay between these two classical mechanisms of synchronization. The original result of the paper is the establishment of the robustness of synchronization when the ants' internal clocks are under the influence of noise. This finding is in support of the autocatalytic ant colony model as a plausible explanation for the observed synchronization in ant nests.

The rest of the paper is organized as follows. In Section 2, we briefly present the autocatalytic ant colony model and write the integro-differential equations that describe the model in the limit of infinite nest sizes (we call these equations mean-field equations, but they are exact in this limit). The equilibrium solutions and their local stability are also discussed in this section. In Section 3, we show that the equilibrium solutions are always stable for exponentially distributed rest periods. In Section 4, we study the more challenging case where the rest period distribution is the zero-truncated Gaussian, and we obtain the regions in parameter space where the periodic solutions appear. Finally, in Section 5, we summarize our results and give some concluding remarks.

2. Mean-Field Equations

The derivation of the mean-field equations governing the dynamics of the autocatalytic ant colony model [10] for colonies of infinite size follows the same line as in the case of fixed rest periods [12]. Each ant can be in one of three possible states: inactive, activatable inactive, and active. An active ant becomes inactive with rate μ and remains in this state for a fixed time $\tau > 0$, which is specified by a probability distribution $p(\tau)$. Each time an ant becomes inactive, a new rest period τ is drawn using the distribution $p(\tau)$. When the rest period is over, the inactive ant deterministically becomes an activatable inactive ant. An activatable inactive ant can either become active spontaneously with a rate of α or, more importantly, can be activated by physical contact with an active ant. The effectiveness of the autocatalytic activation is determined by the activation rate β. Hence, the positive feedback or autocatalytic property of the model. Introducing the notation $a(t)$, $b(t)$, and $s(t)$ for the fractions of active, activatable inactive, and inactive ants, respectively, at time t, we write the equations:

$$\frac{da}{dt} = -\mu a(t) + b(t)[\alpha + \beta a(t)] \tag{1}$$

$$\frac{db}{dt} = -b(t)[\alpha + \beta a(t)] + \mu \int_0^\infty p(\tau) a(t-\tau) d\tau \tag{2}$$

$$\frac{ds}{dt} = \mu \left[a(t) - \int_0^\infty p(\tau) a(t-\tau) d\tau \right] \tag{3}$$

where $a(t) + b(t) + s(t) = 1$. The new ingredient, compared to the equations for fixed τ (i.e., for $p(\tau) = \delta(\tau - \tau_m)$, where $\delta(x)$ is the Dirac delta function) [12], is that the increment to the fraction of inactive ants at time t comes from ants that became inactive at any time before t, properly weighted by the distribution of rest times. Here, $a(t-\tau)$ is the fraction of active ants at time $t-\tau$. Multiplied by the inactivation rate μ, it gives the fraction of ants that have become inactive at time $t-\tau$ and will deterministically wake up at time t. The integral over the probability distribution of rest periods takes into account the fact that each ant is inactive for a period of duration τ drawn from the probability distribution $p(\tau)$.

The mean-field Equations (1)–(3) are almost identical to those used in SIRS models of epidemiology, where individuals can be in three different states, namely, susceptible (S), infected (I), and recovered (R). After infection individuals become immune for a fixed period of time τ and then transition deterministically to the susceptible state [15,16]. Thus, recovered individuals are analogous to inactive ants, infected individuals are analogous to active ants, and susceptible individuals are analogous to activatable inactive ants. The only difference between the two models is that ants can spontaneously self-activate at a rate α, so activity, unlike disease, can reappear even when there are no active ants. However, this is a big difference. At $\alpha = 0$, there is a disease-free equilibrium where the population consists only of susceptible individuals, the stability of which is of primary interest in epidemiological studies. This solution is of no interest in the ant scenario, since activity is aimed at taking care of the brood, and a solution that eliminates the active state means the death of the colony.

We note that although both fractional differential Equations (FDE) and integro-differential Equations (IDE) can be used to model systems in which the current state depends on the past history and the present state, FDE describes systems with nonlocal effects, i.e., the value of the derivative at a point depends on the values of the function over an interval [17]. This is not the case for the autocatalytic ant colony model, which was originally introduced and studied using Monte Carlo simulations [10], so the classical IDE approach is appropriate [18].

Let us first consider the fixed point or equilibrium solutions $a^* = a(t)$, $b^* = b(t)$ and $s^* = s(t)$ of these equations, which are obtained by setting the time derivatives to zero. This procedure yields:

$$b^* = \frac{\mu a^*}{\alpha + \beta a^*}, \tag{4}$$

and so, we need one more equation to determine the equilibrium solution unambiguously, since $a^* + b^* + s^* = 1$. The additional equation is found by integrating Equation (3) from 0 to T:

$$\int_0^T \frac{ds}{dt} dt = \mu \left[\int_0^T a(t) dt - \int_0^T dt \int_0^\infty d\tau p(\tau) a(t - \tau) \right], \tag{5}$$

which, after some simple arithmetic, can be rewritten as:

$$s(T) - s(0) = \mu \int_0^T a(t) dt - \mu \int_0^\infty d\tau p(\tau) \int_{-\tau}^{T-\tau} a(u) du. \tag{6}$$

We note that for $t \in [-\tau, 0)$ the fraction of active ants $a(t)$ is given by the initial conditions, which in turn determines the fraction of inactive ants at $t = 0$, namely:

$$s(0) = \mu \int_0^\infty d\tau p(\tau) \int_{-\tau}^0 a(u) du, \tag{7}$$

assuming that $s(-\tau) = 0$. Using this result in Equation (6), we obtain:

$$\begin{aligned} s(T) &= \mu \int_0^T a(t) dt - \mu \int_0^\infty d\tau p(\tau) \int_0^{T-\tau} a(u) du \\ &= \mu \int_0^\infty d\tau p(\tau) \int_{T-\tau}^T a(u) du. \end{aligned} \tag{8}$$

Next, we assume that the distribution of rest periods is such that $p(\tau) \to 0$ when $\tau \to \infty$ so that we can take the limit $T \to \infty$ and guarantee that $T - \tau \to \infty$ as well. In this case, we can replace $a(u)$ in the integrand of Equation (8) by its equilibrium value:

$$\lim_{T \to \infty} s(T) = \mu \lim_{T \to \infty} \int_0^\infty d\tau p(\tau) \int_{T-\tau}^T a(u) du = \mu a^* \int_0^\infty d\tau \tau p(\tau), \tag{9}$$

and obtain:

$$s^* = \mu a^* \langle \tau \rangle \tag{10}$$

regardless of our choice for $a(t)$ in the range $t \in [-\tau, 0)$. Thus, with respect to the values of the fixed points, selecting rest periods from a distribution $p(\tau)$ yields the same results as a fixed rest period set to the mean of that distribution. Equation (10) shows that at equilibrium, active ants become inactive at the rate μ and remain inactive on average for the period $\langle \tau \rangle$.

Finally, using Equations (4) and (10) together with the normalization condition allows us to write an equation for the fraction of active ants at equilibrium:

$$\beta(1 + \mu\langle\tau\rangle)(a^*)^2 + [\alpha(1 + \mu\langle\tau\rangle) + \mu - \beta] a^* - \alpha = 0, \tag{11}$$

which always has one negative root and one positive root less than 1. The important point here is that for all values of the model parameters, Equations (4), (10) and (11) always produce valid equilibrium solutions, i.e., a^*, b^*, and s^* are positive and less than 1.

In the case $\alpha = 0$, which is the focus of epidemiological studies, Equation (4) gives $b^* = \mu/\beta$, and Equation (11) gives:

$$a^* = \frac{\beta - \mu}{\beta(1 + \mu\langle\tau\rangle)} \tag{12}$$

if $\beta > \mu$. If $\beta \leq \mu$, we have $b^* = 1$ and $a^* = 0$, which corresponds to a disease-free scenario. We can easily show that a^*, i.e., the positive root of the quadratic Equation (11), is a monotonously increasing function of α, since $da^*/d\alpha = 0$ only for $\mu = 0$, and in the limit $\alpha \to \infty$ we have:

$$a^* = \frac{1}{1 + \mu\langle\tau\rangle}, \tag{13}$$

which is greater than a^* calculated at $\alpha = 0$, given in Equation (12). The result that $da^*/d\alpha > 0$ will be of great value in analyzing the stability of the equilibrium solutions.

In summary, choosing the rest periods τ from a probability distribution has no effect on the values of the equilibrium solutions, which are determined solely by the mean $\langle\tau\rangle$. However, the randomness has a strong effect on their stability, as we will show next.

The analysis of the stability of the fixed point solutions is standard [19] and involves the linearization of Equations (1) and (3) for the equilibrium values a^* and s^* by writing $a(t) = a^* + \epsilon_a(t)$ and $s(t) = s^* + \epsilon_s(t)$ and looking for solutions of the form $\epsilon_a(t) = \epsilon_a(0)e^{\lambda t}$ and $\epsilon_s(t) = \epsilon_s(0)e^{\lambda t}$, where $\epsilon_a(0) \ll 1$ and $\epsilon_s(0) \ll 1$ are constants. These solutions exist if the eigenvalues λ satisfy the following characteristic equation:

$$\lambda(\lambda + X) + \left(1 - \langle e^{-\lambda\tau}\rangle\right)Y = 0, \tag{14}$$

where:

$$X = \mu - \beta + \alpha + \beta a^*(2 + \mu\langle\tau\rangle) \tag{15}$$

and

$$Y = \mu(\alpha + \beta a^*) \tag{16}$$

are auxiliary variables.

Let us first consider the real solutions of Equation (14). Note that $Y \geq 0$, so if $X \geq 0$ too, only negative real solutions for λ are possible. Of course, the conclusion that $X \geq 0$ follows immediately if $\mu \geq \beta$, so the tricky case is $\mu < \beta$. Since X is a monotonically increasing function of α, it is bounded from below by its value at $\alpha = 0$, which is easily obtained using Equation (12) and yields $X = (\beta - \mu)/(1 + \mu\langle\tau\rangle) > 0$. Therefore, $X \geq 0$ for all α and we conclude that Equation (14) has only negative real solutions.

Thus, we need to look for the complex solutions of Equation (14). We recall that the fixed point solution is unstable if $\mathrm{Re}(\lambda) > 0$, In fact, by writing $\lambda = u + iv$, where u and v are real variables, and using Euler's formula, we can easily show that if u and v are a solution, then so are u and $-v$, so we can consider $v > 0$ without loss of generality. In addition, $u = v = 0$ (i.e., $\lambda = 0$) is a solution. The challenge then is to write down and solve the equations for the real and imaginary parts of λ, given the distribution $p(\tau)$. This will be done next for two choices of the rest period distribution.

Finally, we note that for $\alpha = 0$ and $\beta \leq \mu$ the solution $b^* = 1$ and $a^* = 0$ is locally stable regardless of the choice of $p(\tau)$, since $\lambda = \beta - \mu \leq 0$. This is an important result because increasing α increases the region of stability of the fixed-point solutions [12], as expected, since spontaneous activation begins to compete with the mechanism of activation by contact between ants, which is one of the two key ingredients to produce synchronization in the autocatalytic ant colony model (the other being the rest period) [10]. Therefore, for $\beta \leq \mu$, there are no period solutions to the mean-field equations regardless of the value of α and the choice of $p(\tau)$.

3. Exponential Distribution

Here, we consider the case where the rest times τ are distributed by the exponential distribution with rate parameter γ:

$$p(\tau) = \gamma \exp(-\gamma\tau). \tag{17}$$

Thus, $\langle\tau\rangle = 1/\gamma$ and $\langle e^{-\lambda\tau}\rangle = \gamma/(\gamma + \lambda)$. The nonzero eigenvalues λ are the roots of the quadratic equation:

$$\lambda^2 + \lambda(X + \gamma) + Y + \gamma X = 0. \tag{18}$$

Since we have already proved for a general distribution $p(\tau)$ that the real solutions are negative, we only need to consider the complex solutions of Equation (18). In this case, we have $\mathrm{Re}(\lambda) = -(X + \gamma)/2 < 0$ since $X \geq 0$, as shown before. Thus, the equilibrium solutions are always stable for exponentially distributed rest periods.

4. Zero-Truncated Normal Distribution

We need a distribution where the mean and the variance of the rest periods are independent variables as in the Gaussian distribution. Since τ must be nonnegative, a good candidate is the zero-truncated normal distribution [20]:

$$p(\tau) = \frac{2}{\mathrm{erfc}\left(-\tau_m/\sqrt{2\sigma^2}\right)} \frac{1}{\sqrt{2\pi\sigma^2}} \exp\left[-(x-\tau_m)^2/2\sigma^2\right] \tag{19}$$

for $\tau \geq 0$. The mean value, which is necessary for the calculation of the equilibrium solutions, is:

$$\langle\tau\rangle = \tau_m + \frac{2\sigma^2}{\mathrm{erfc}\left(-\tau_m/\sqrt{2\sigma^2}\right)} \frac{1}{\sqrt{2\pi\sigma^2}} \exp\left(-\tau_m^2/2\sigma^2\right), \tag{20}$$

and the Laplace transform, which appears in Equation (14), is:

$$\langle e^{-\lambda\tau}\rangle = \frac{1}{\mathrm{erfc}\left(-\tau_m/\sqrt{2\sigma^2}\right)} \exp[-\lambda\tau_m + \lambda^2\sigma^2/2] \mathrm{erfc}\left[(\lambda\sigma^2 - \tau_m)/\sqrt{2\sigma^2}\right]. \tag{21}$$

The advantage of the distribution (19) is that the fixed-point analysis reduces to the case of fixed τ (i.e., $p(\tau) = \delta(\tau - \tau_m)$) when $\sigma^2 \to 0$, so we can check the robustness of the results for fixed $\tau = \tau_m$ against noise, which is measured by the parameter σ^2.

The equations for the real and imaginary parts of the eigenvalue $\lambda = u + iv$ are:

$$u^2 - v^2 + uX + Y - Y\mathrm{Re}(\langle e^{-\lambda\tau}\rangle) = 0 \tag{22}$$

$$2uv + vX - Y\mathrm{Im}(\langle e^{-\lambda\tau}\rangle) = 0, \tag{23}$$

where Laplace transform (21) can be written explicitly in terms of u and v as:

$$\langle e^{-\lambda\tau}\rangle = \frac{\exp[-u\tau_m + (u^2 - v^2)\sigma^2/2]}{\mathrm{erfc}\left(-\tau_m/\sqrt{2\sigma^2}\right)} \exp\left[iv(u\sigma^2 - \tau_m)\right] \mathrm{erfc}\left[\frac{u\sigma^2 - \tau_m}{\sqrt{2\sigma^2}} + i\frac{v\sigma^2}{\sqrt{2\sigma^2}}\right]. \tag{24}$$

Although there is no explicit analytical expression for the real and imaginary parts of the error function, there is an excellent numerical approximation (see Equation 7.1.29 of [21]):

$$\mathrm{Re}[\mathrm{erf}(x+iy)] = \mathrm{erf}(x) + \frac{e^{-x^2}}{2\pi x}(1 - \cos 2xy) + \frac{2}{\pi} e^{-x^2} \sum_{k=1}^{\infty} \frac{e^{-k^2/4}}{k^2 + 4x^2} f_k(x,y) \tag{25}$$

$$\mathrm{Im}[\mathrm{erf}(x+iy)] = \frac{e^{-x^2}}{2\pi x} \sin 2xy + \frac{2}{\pi} e^{-x^2} \sum_{k=1}^{\infty} \frac{e^{-k^2/4}}{k^2 + 4x^2} g_k(x,y), \tag{26}$$

where:

$$f_k(x,y) = 2x - 2x\cos 2xy \cosh ky + k \sin 2xy \sinh ky \tag{27}$$

and

$$g_k(x,y) = 2x \sin 2xy \cosh ky + k \cos 2xy \sinh ky. \tag{28}$$

Remarkably, the error of this approximation is less than 10^{-16} for all x and y [21]. Defining $x = (u\sigma^2 - \tau_m)/\sqrt{2\sigma^2}$ and $y = v\sigma^2/\sqrt{2\sigma^2}$ we write:

$$\begin{aligned} \mathrm{Re}(\langle e^{-\lambda\tau}\rangle) = {} & \frac{\exp[-u\tau_m + (u^2 - v^2)\sigma^2/2]}{\mathrm{erfc}\left(-\tau_m/\sqrt{2\sigma^2}\right)} \Big[\mathrm{Im}[\mathrm{erf}(x+iy)] \sin v(u\sigma^2 - \mu) \\ & + (1 - \mathrm{Re}[\mathrm{erf}(x+iy)]) \cos v(u\sigma^2 - \mu)\Big] \end{aligned} \tag{29}$$

and

$$\mathrm{Im}(\langle e^{-\lambda\tau}\rangle) = \frac{\exp[-u\tau_m+(u^2-v^2)\sigma^2/2]}{\mathrm{erfc}\left(-\tau_m/\sqrt{2\sigma^2}\right)}\Big[-\mathrm{Im}[\mathrm{erf}(x+iy)]\cos v(u\sigma^2-\mu) + (1-\mathrm{Re}[\mathrm{erf}(x+iy)])\sin v(u\sigma^2-\mu)\Big], \tag{30}$$

so that we can easily calculate all quantities that appear in Equations (22) and (23).

In the case of fixed τ, it is possible to write v explicitly in terms of u (see Appendix A), but this is clearly impossible for the zero-truncated normal distribution (19). However, Equations (22) and (23) can be solved in a simple way: for fixed u, we solve Equation (22) for v using a bisection method, so that Equation (23) depends only on u and can be solved by a second bisection.

Figure 1 shows the resulting values of u as a function of the noise parameter σ^2, which is the control parameter of interest. In the left panel, we fix τ_m and show u for several values of the activation rate β. The important result is that u decreases with increasing σ^2 and eventually becomes negative when σ^2 is greater than a threshold. Since we associate the instability regime of the fixed-point solutions (i.e., $u > 0$) with the oscillatory solutions, increasing the variability of the rest periods by increasing σ^2 beyond the threshold eliminates the synchronized rhythmic activity. Although these results give the impression that increasing β tends to destabilize the equilibrium solutions (i.e., u seems to increase with β for fixed σ^2), this is not the case. In fact, u is not a monotonically increasing function of β and, for example, u becomes negative for $\beta > 4.9$ when $\sigma^2 = 4$ (see Figure 2). In the right panel of Figure 1, we fix β and vary τ_m to emphasize that the stability of the fixed-point solutions depends on the parameters τ_m and σ^2 separately, and not only on the coefficient of variation, whose square is σ^2/τ_m^2. This panel also shows that there is a minimum value τ_m below which the fixed-point solutions are stable, regardless of the value of the noise parameter σ^2. This minimum value is obtained by setting $\sigma^2 = 0$.

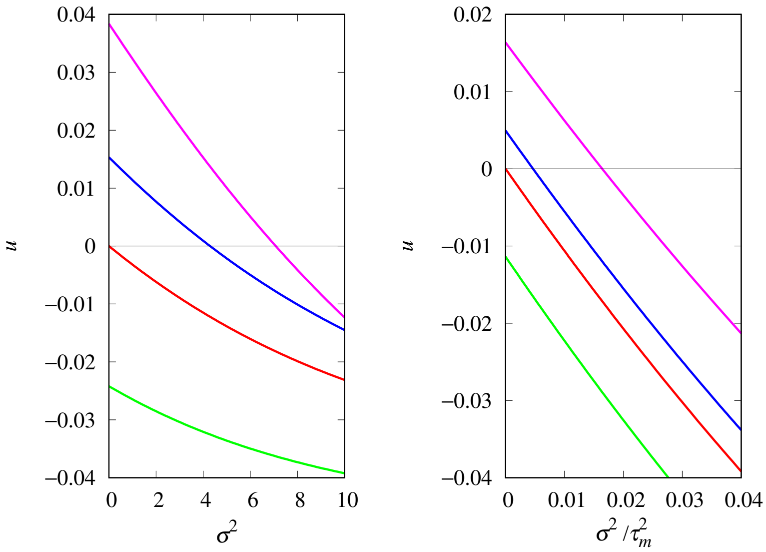

Figure 1. (**Left**) Real part u of the eigenvalue λ as a function of the parameter σ^2 of the truncated normal distribution (19) with $\tau_m = 10$ and (top to bottom) $\beta = 3, 2, 1.748$, and 1.5. (**Right**) u as a function of the ratio σ^2/τ_m^2 with $\beta = 4$ and (top to bottom) $\tau_m = 5.5, 5, 4.828$, and 4.5. The fixed-point solutions are unstable if $u > 0$. The other parameters are $\mu = 1$ and $\alpha = 0.002$.

Figure 2 shows the regions in the parameter plane (τ_m, β), where the fixed-point solutions are unstable for $\sigma^2 = 0$ and $\sigma^2 = 4$. The figure reveals two remarkable features. First, there is a minimum value of τ_m below which the fixed-point solutions are stable regardless of the value of β, and this minimum increases with the noise parameter σ^2.

Second, there is a minimum value of the activation rate β below which the fixed-point solutions are stable no matter how large τ_m is. Specifically, for the data in the figure, this minimum is $\beta \approx 1.41$ and occurs for $\tau_m \approx 25$ (we recall that for $\alpha = 0$, the minimum is $\beta = \mu$). The lower boundary of the shaded region is practically not affected by the variation of σ^2. Somewhat surprisingly, too large values of β also lead to the stability of the fixed-point solutions. This is interesting because the parameter $\beta > 0$ is central to the functionality of the autocatalytic ant colony model to produce periodic oscillations, since it controls the activation of ants by contact with active ants [10]. Too few (effective) contacts will fail to synchronize the activity of the ants, as expected, but too many (effective) contacts will fail as well. Therefore, there is an intricate interplay between the model parameters necessary to maintain the periodic solutions. As expected, increasing σ^2 leads to a shrinking of the region of existence of periodic solutions.

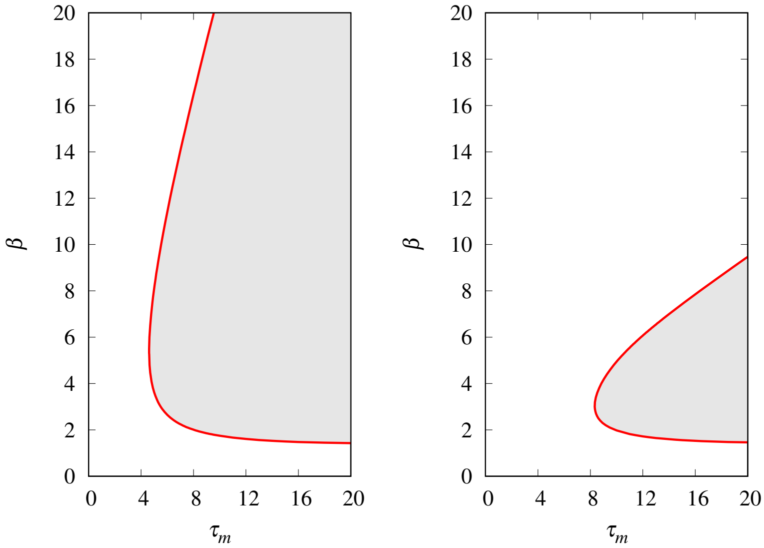

Figure 2. Values of the activation rate β and the parameter τ_m of the truncated normal distribution (19) (shaded region) for which the fixed-point solutions are unstable andthus mean-field equations exhibit periodic solutions. (**Left**) $\sigma^2 = 0$. (**Right**) $\sigma^2 = 4$. The other parameters are $\mu = 1$ and $\alpha = 0.002$.

Figures 3 and 4 show the results of the numerical solution of the mean-field Equations (1)–(3) for $\sigma^2 = 4$ and parameters in representative regions of the stability analysis, summarized in the right panel of Figure 2. In particular, Figure 3 shows the effect of increasing τ_m for fixed β. For small τ_m we observe an oscillatory convergence to the fixed-point solution a^*, but for τ_m in the region of instability of the equilibrium solution, we observe periodic solutions with period greater than τ_m. In fact, an ant should go through three states in a cycle: inactive, which lasts τ_m on average, activatable inactive, which is bounded by $1/\alpha$, and active, which lasts $1/\mu$ on average. Thus, the period of the oscillations must be greater than τ_m. However, the amplitude of the oscillations is remarkably insensitive to increasing τ_m. For example, the amplitude for $\tau_m = 100$ is the same as for $\tau_m = 20$ shown in the figure. The amplitude increases with decreasing σ^2, but the peak of activity does not go beyond $a = 0.4$. An important feature here is that the periodic solutions do not oscillate around the unstable fixed point as in the case of conservative (e.g., Lotka–Volterra) systems [19,22]. Moreover, for large τ_m, the fractions of active and activatable inactive ants vanish for some of the time periods and of course become nonzero when the ants wake up from their rest periods. Figure 4 shows a similar analysis but with fixed τ_m and increasing β. The results confirm the findings of the stability analysis that the periodic solutions appear only for intermediate values of the activation rate.

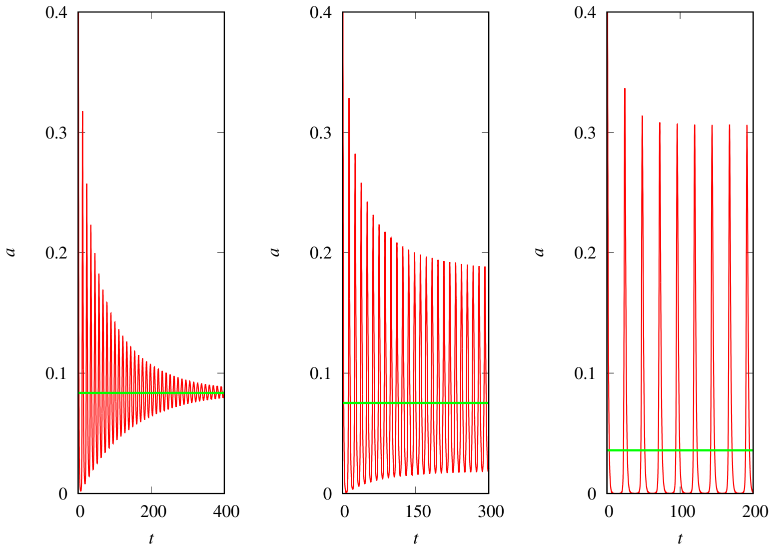

Figure 3. Fraction of active ants $a(t)$ as a function of time t for (**Left**) $\tau_m = 8$, (**Middle**) $\tau_m = 9$, and (**Right**) $\tau_m = 20$. The horizontal lines indicate the values of the fixed point a^*. The other parameters are $\beta = 4$, $\sigma^2 = 4$, $\alpha = 0.002$, and $\mu = 1$. The fixed-point solutions are unstable for $\tau_m > 8.84$.

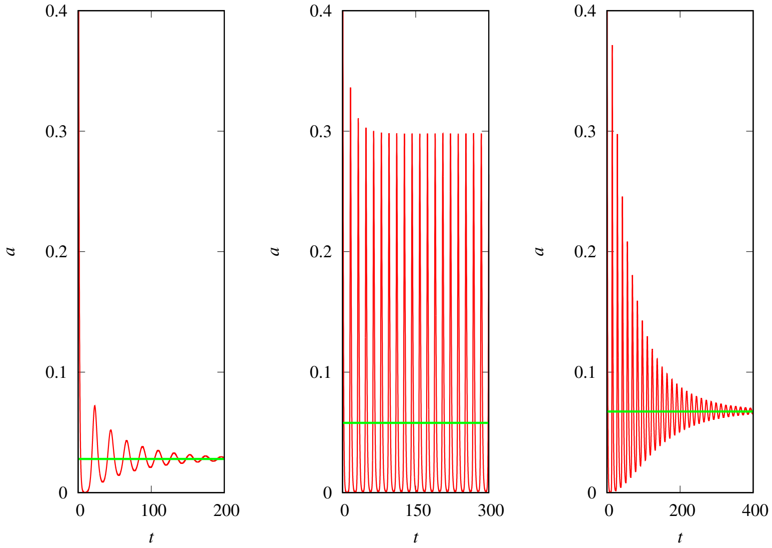

Figure 4. Fraction of active ants $a(t)$ as a function of time t for (**Left**) $\beta = 1.5$, (**Middle**) $\beta = 4$, and (**Right**) $\beta = 8$. The horizontal lines indicate the values of the fixed point a^*. The other parameters are $\tau_m = 12$, $\sigma^2 = 4$, $\alpha = 0.002$, and $\mu = 1$. The fixed-point solutions are unstable for $1.72 < \beta < 6.05$.

While the intuition for the nonexistence of periodic solutions for small β is clear—an active ant is likely to become inactive before activating an activatable inactive ant, reducing the effectiveness of the autocatalytic activation synchronization mechanism—we have no intuition to explain the nonexistence of periodic solutions for large β as well. In fact, for large β, activation is so effective that there are no ants in the inactive activatable state (more precisely, $b(t)$ vanishes with $1/\beta$ for any t), and the mean-field equations reduce to a single linear integro-differential equation:

$$\frac{da}{dt} = -\mu \left[a(t) - \int_0^\infty p(\tau) a(t-\tau) d\tau \right], \tag{31}$$

describing the scenario of independent ants sleeping at rate μ and becoming active after a period of time τ. The equation for the real part u of the eigenvalue of the characteristic equation is:

$$u = -\mu\left[1 - \int_0^\infty p(\tau)e^{-u\tau}\cos(v\tau)d\tau\right], \tag{32}$$

which has no solution with $u > 0$, since the rhs of this equation is always negative for $u > 0$.

At this point, we can finally show a result that we have mentioned several times before, namely that for independent (i.e., noninteracting) ants, the equilibrium solutions are always stable. Setting $\beta = 0$ in Equations (15) and (16) yields $X = \mu + \alpha$ and $Y = \mu\alpha$, so the characteristic Equation (14) does not depend on the equilibrium solutions. In the Appendix A, we show that this characteristic equation has no solutions with positive real part for $\sigma^2 = 0$. Since our analysis of the zero-truncated Gaussian distribution shows that if the equilibrium solution is stable for $\sigma^2 = 0$, it is also stable for $\sigma^2 > 0$, we can rule out the possibility of periodic solutions in the case of noninteracting ants, demonstrating the key role of the contagious activation mechanism in generating periodic oscillations.

5. Discussion

The mathematical analysis of the autocatalytic ant colony model, introduced in the late 1980s to explain bursts of synchronized activity in ant nests [10], points to two key mechanisms for their existence: the activation of inactive but awake (i.e., immobile) ants by physical contact with active ants, and the resting period of inactive (sleeping) ants [12]. The effectiveness of the first mechanism is measured by the activation rate β, and that of the second by the rest period τ. However, by itself, none of these mechanisms can produce periodic solutions of the mean-field Equations (1)–(3), since setting $\beta = 0$ or neglecting the rest period leads to the stability of the equilibrium solutions, i.e., the fixed points.

These key mechanisms are subject to noise, and understanding their robustness to noise is essential to justify the relevance of the model to explain synchronized bursts of activity in ant nests. In fact, spontaneous activation, as measured by the parameter α, acts as noise to the contagious activation mechanism and can disrupt synchronization if it is large enough [12]. It is interesting to note that for $\alpha = 0$, the equations describing the autocatalytic ant colony model reduce to those used in SIRS models in epidemiology, where individuals become immune for a fixed period of time and transition deterministically to the susceptible state [15,16]. Setting spontaneous activation to zero makes sense in the epidemiological context because it allows for the possibility of a disease-free solution, but in the ant model, the focus is instead on maintaining a periodic active state. Our focus here was on the effect of noise on the rest period τ, rather than on the contagious activation mechanism.

We show that for exponentially distributed rest periods, the equilibrium solutions are always stable. The reason for this may be that the coefficient of variation (i.e., the ratio of the standard deviation to the mean) for the exponential distribution (17) is 1, which may be too much noise to maintain the delicate balance needed to stabilize the periodic solutions. For the zero-truncated exponential distribution (19), we find regions in the parameter space where periodic solutions exist. As the noise parameter σ^2 increases, this region shrinks and moves into the region of large τ_m to keep the coefficient of variation small, as shown in Figure 2. Note, however, that even for a fixed distribution of rest periods, the stability of the equilibrium solutions is not determined solely by the coefficient of variation, as shown in Figure 1, since the fixed points depend only on the mean rest period.

We emphasize that we have shown analytically that the equilibrium solutions are unstable in certain regions of the parameter space (see Figure 2). The solutions of the mean-field Equations (1)–(3) in these regions were obtained numerically and always resulted to be stable limit cycles (see, e.g., Figures 3 and 4), but we have no proof of this result. However, since in the epidemiological scenario (i.e., for $\alpha = 0$), the existence of locally asymptotically stable periodic solutions has been proved using Hopf bifurcation techniques [15], we expect the same conclusion to hold for our model. This is a challenging topic for future research.

Although the autocatalytic ant colony model successfully reproduces qualitatively the oscillatory activity pattern observed in the nest of some ant species, there is at least one quantitative feature that the model fails to reproduce, namely, that a burst of activity involves almost the entire nest population [3]. In the deterministic model studied here, the maximum activity we find involves about 40% of the population, and this activity peak decreases with increasing noise. The activity peaks may be higher in finite populations due to the coherence resonance effect, which prevents the decrease in amplitude of the damped oscillations that would eventually bring the dynamics to the deterministic equilibrium [23,24]. Perhaps this stochastic effect can also contribute to increasing the amplitude of the oscillations in the case of unstable equilibrium solutions. Testing this possibility, as well as searching for the model features that produce higher activity peaks using a group selection approach, similar to what was done to evolve response thresholds [25], is a promising direction for future research.

Author Contributions: Conceptualization, J.F.F.; formal analysis, P.M.M.d.S. and J.F.F.; investigation, P.M.M.d.S. and J.F.F.; methodology, J.F.F.; supervision, J.F.F.; validation, P.M.M.d.S.; writing—original draft, J.F.F.; writing—review and editing, P.M.M.d.S. and J.F.F. All authors have read and agreed to the published version of the manuscript.

Funding: J.F.F. is partially supported by the Conselho Nacional de Desenvolvimento Científico e Tecnológico grant number 305620/2021-5. P.M.M.d.S. is supported by the Coordenação de Aperfeiçoamento de Pessoal de Nível Superior—Brasil (CAPES)—Finance Code 001.

Data Availability Statement: Data will be made available on request.

Conflicts of Interest: The authors declare no conflicts of interest. The funders had no role in the design of the study; in the collection, analyses, or interpretation of data; in the writing of the manuscript; or in the decision to publish the results.

Appendix A

Here, we show that the equilibrium solutions are stable in the case of noninteracting ants (i.e., $\beta = 0$). In fact, for $\beta = 0$ and $p(\tau) = \delta(\tau - \tau_m)$ the characteristic Equation (14) is:

$$\lambda(\lambda + \mu + \alpha) + \left(1 - e^{-\lambda\tau_m}\right)\mu\alpha = 0. \tag{A1}$$

This equation is rewritten in terms of the real and imaginary parts of the eigenvalue $\lambda = u + iv$ as:

$$\begin{aligned} u^2 - v^2 + u(\mu + \alpha) + \mu\alpha &= \mu\alpha e^{-u\tau_m}\cos(v\tau_m) && \text{(A2)} \\ 2uv + v(\mu + \alpha) &= -\mu\alpha e^{-u\tau_m}\sin(v\tau_m). && \text{(A3)} \end{aligned}$$

Squaring and adding these equations yield:

$$v^4 + bv^2 + c = 0 \tag{A4}$$

where:

$$b = 2u(u + \mu + \alpha) + \mu^2 + \alpha^2 \tag{A5}$$

and

$$c = u^2(u + \mu + \alpha)^2 + 2\mu\alpha u(u + \mu + \alpha) + \mu^2\alpha^2\left(1 - e^{-2u\tau_m}\right). \tag{A6}$$

If $u > 0$, we have $b > 0$ and $c > 0$, so Equation (A4) has no real solutions for v. Therefore, $u = \mathrm{Re}(\lambda) \leq 0$ and the equilibrium solution:

$$a^* = \frac{\alpha}{\mu + \alpha + \mu\alpha\tau_m} \tag{A7}$$

is stable for $\beta = 0$. Note that it is also possible to obtain a quartic equation for v in the case $\beta > 0$, provided that τ is fixed [12].

References

1. Strogatz, S.H. *Sync: How Order Emerges from Chaos in the Universe, Nature, and Daily Life*; Hachette Books: New York, NY, USA, 2004.
2. Sumpter, D.J.T. *Collective Animal Behavior*; Princeton University Press: Princeton, NJ, USA, 2010.
3. Franks, N.R.; Bryant, S.; Griffiths, R.; Hemerik, L. Synchronization of the behaviour within nests of the ant Leptothorax acervorum (Fabricuis)—I. Discoveringt he phenomenon and its relation to the level of starvation. *Bull. Math. Biol.* **1990**, *52*, 597–612.
4. Cole, B.J. Short-Term Activity Cycles in Ants: Generation of Periodicity by Worker Interaction. *Am. Nat.* **1991**, *137*, 244–259. [CrossRef]
5. Tennenbaum, M.; Fernandez-Nieves, A. Activity-driven changes in the mechanical properties of fire ant aggregations. *Phys. Rev. E* **2017**, *96*, 052601. [CrossRef] [PubMed]
6. Doering, G.N.; Drawert, B.; Lee, C.; Pruitt, J.N.; Petzold, L.R.; Dalnoki-Veress, K. Noise resistant synchronization and collective rhythm switching in a model of animal group locomotion. *R. Soc. Open Sci.* **2022**, *9*, 211908. [CrossRef] [PubMed]
7. Hatcher, M.J.; Tofts, C.; Franks, N.R. Mutual exclusion as a mechanism for information exchange within ant nests. *Naturwissenschaften* **1992**, *79*, 32–34. [CrossRef]
8. Doering, G.N.; Lee, C.L.; Dalnoki-Veress, K. Synchronized locomotion can improve spatial accessibility inside ant colonies. *Proc. R. Soc. Lond. Ser. B Biol. Sci.* **2023**, *290*, 20231805. [CrossRef] [PubMed]
9. Strogatz, S.H.; Stewart, I. Coupled oscillators and biological synchronization. *Sci. Am.* **1993**, *269*, 102–109. [CrossRef] [PubMed]
10. Goss, S.; Deneubourg, J.L. Autocatalysis as a source of synchronised rhythmical activity in social insects. *Insectes Soc.* **1988**, *35*, 310–315. [CrossRef]
11. Tofts, C.; Hatcher, M.; Franks, N.R. The Autosynchronization of the Ant Leptothorax acervorum (Fabricius): Theory, Testability and Experiment. *J. Theor. Biol.* **1992**, *157*, 71–82. [CrossRef]
12. da Silveira, P.M.M.; Fontanari, J.F. A soluble model for synchronized rhythmic activity in ant colonies. *Math. Biosci.* **2024**, *375*, 109245. [CrossRef] [PubMed]
13. Hemerik, L.; Franks, N.R.; Britton, N. Synchronization of the behaviour within nests of the ant Leptothorax acervorum (Fabricius)—II. Modelling the phenomenon and predictions from the model. *Bull. Math. Biol.* **1990**, *52*, 613–628.
14. Porfiri, M.; Abaid, N.; Garnier, S. Socially driven negative feedback regulates activity and energy use in ant colonies. *PLoS Comput. Biol.* **2024**, *20*, e1012623. [CrossRef] [PubMed]
15. Hethcote, H.W.; Stech, H.W.; Van Den Driessche, P. Nonlinear Oscillations in Epidemic Models. *SIAM J. Appl. Math.* **1981**, *40*, 1–9. [CrossRef]
16. Gonçalves, S.; Abramson, G.; Gomes, M.F.C. Oscillations in SIRS model with distributed delays. *Eur. Phys. J. B* **2011**, *81*, 363–371. [CrossRef]
17. Diethelm, K. *The Analysis of Fractional Differential Equations*; Springer: New York, NY, USA, 2010.
18. Hale, J.K. *Theory of Functional Differential Equations*; Springer: New York, NY, USA, 1977.
19. Murray, J.D. *Mathematical Biology: I. An Introduction*; Springer: New York, NY, USA, 2007.
20. Robert, C.P. Simulation of truncated normal variables. *Stat. Comput.* **1995**, *5*, 121–125. [CrossRef]
21. Abramowitz, M.; Stegun, I.A. *Handbook of Mathematical Functions*; Dover Publications: New York, NY, USA, 1972.
22. Britton, N.F. *Essential Mathematical Biology*; Springer: London, UK, 2003.
23. McKane, A.J.; Newman, T.J. Predator-prey cycles from resonant amplification of demographic stochasticity. *Phys. Rev. Lett.* **2005**, *94*, 218102. [CrossRef] [PubMed]
24. Kuske, R.; Gordillo, L.F.; Greenwood, P. Sustained oscillations via coherence resonance in SIR. *J. Theor. Biol.* **2007**, *245*, 459–469. [CrossRef] [PubMed]
25. Fontanari, J.F.; Oliveira, V.M.; Campos, P.R.A. Evolving division of labor in a response threshold model. *Ecol. Complex.* **2024**, *58*, 101083. [CrossRef]